Soil Water Stress Overrides the Boosting Effect of iWUE from Rising CO_2 and temperature in Determining Plantation Mortality in Semi-arid Cold Area

Guodong Jia[a,b*], Lixin Chen[a,b], Xinxiao Yu[a,b*], Ziqiang Liu[c]

[a] Key Laboratory of State Forestry Administration on Soil and Water Conservation, Beijing Forestry University, Beijing 100083, China

[b] School of Soil and Water Conservation, Beijing Forestry University, Beijing 100083, China

[c] School of Forestry, Nanjing Forestry University, Nanjing 210037, China

*Corresponding authors Email addresses: jiaguodong@bjfu.edu.cn; yuxinxiao111@163.com

Abstract

The counteractive influence of atmospheric CO_2 enrichment and drought stress on tree growth results in great uncertainty in growth patterns of planted forests in cold semi-arid regions. We used tree-ring chronology and carbon isotope analysis to track ecophysiological processes in reaction to environmental factors over the past four decades of *Populus simonii* plantations in cold semi-arid areas in northern China. Our results showed that the boosting effect of the rising atmospheric CO_2 concentration (C_a) on iWUE and stem growth was more significant in declined stands. However, the increased iWUE did not negate tree dieback when water stress was present. Therefore, the BAI and iWUE deviation of different health status trees started from a very early age. Climatic factors showed limited influences on the stem growth of the poplar plantations. The inaccessibility of deep soil water due to site-specific soil conditions rendered the trees exposed to chronic soil water stress and constrained stomatal conductance and reduced the CO_2 fertilization effect. Consequently, these stands experienced a lower stem growth rate. In summary, we suggest that soil moisture conditions the iWUE and growth sensitivity to global warming and thus portrays site-specific decline episodes of different degrees in drought-prone areas.

Keywords: tree dieback, dendrochronology, soil water use profile, isotope, planted forests, climate change

Introduction

Increasing drought severity and frequency, due to global warming, has led to vegetation mortality in many regions of the world (N. G. McDowell, Allen, & Marshall, 2010). Functional and structural changes driven by mortality in the ecosystem will cause hydrological changes (Newman et al., 2006), carbon storage reduction (Breshears & Allen, 2002; Kurz et al., 2008), and ecotone conversions (Allen & Breshears, 1998). However, the influence of global warming seems to be a double-edged sword regarding vegetation dynamics in cold regions. Rising atmospheric CO_2 concentration (C_a) and temperature has driven significant changes of vegetation dynamics in cold regions in terms of distribution patterns (Wei et al., 2020) and phenology e.g. (Shen et al., 2019). Plants in such areas are adapted to low temperature conditions and a short growing season, which makes them benefit from increasingly warmer climates. In addition, decades of increasing C_a have been proven to boost vegetation growth by stimulating intrinsic water-use efficiency iWUE (McCarroll & Loader, 2004; Reed, Ballantyne, Cooper, & Sala, 2018). Meanwhile, previous studies indicated that global warming has begun to afflict the semi-arid and arid regions with increasing drought frequency (Fu, 2007; Huang, Guan, & Ji, 2012). The aridity trend thus renders the fragile ecosystems in such areas as the most sensitive areas under the scenario of global warming (Rotenberg & Yakir, 2010). Therefore, understanding the responses of forest ecosystems in cold semi-arid regions under this scenario, provides valuable references for understanding and predicting vegetation patterns in these climatically sensitive areas.

Rising C_a enhance tree growth through improved photosynthesis, also known as the "CO_2 fertilization hypothesis" (Norby et al., 2005). It might also lead to reduced stomatal conductance, and thus enhancing the iWUE. Greater iWUE is of crucial importance in water-limited plant

communities because it alleviates water stress and prolongs the growing season. However, the prevailing increasing in iWUE does not necessarily translate to enhanced tree growth, for example, in cold and arid boreal forests (Dietrich et al., 2016), Mediterranean regions (Fernández-de-Uña, McDowell, Cañellas, & Gea-Izquierdo, 2016) and even tropic areas (van der Sleen et al., 2015). Global meta-analyses attribute the insignificant effect of CO_2 enrichment on tree growth to water stress and nutrient deficiency (Peñuelas, Canadell, & Ogaya, 2011; Silva, Anand, & Leithead, 2010). Under drought stress, plants die of hydraulic failure, carbon starvation, or simplistic limitations (N. McDowell et al., 2008). With warming temperature, atmospheric moisture stress posed by rising vapor pressure deficit (*VPD*) is becoming increasingly crucial to plant performance and survival (Allen, Breshears, & McDowell, 2015; Williams et al., 2013). Recent global forest mortality cases are evidence of the drought constraint over the boosting effect of CO_2 on tree growth (Raffa et al., 2008; Suarez, Ghermandi, & Kitzberger, 2004) and potential association with increased air temperatures (Breshears et al., 2005; Van Mantgem et al., 2009). Therefore, understanding the hydro-carbon mechanisms of tree growth lays the foundation for improving the accuracy of forecasting forest mortality under the scenario of climate change. In addition, investigation of climatic interference on tree growth in response to enriching C_a is necessary to predict forest dynamics in cold semi-arid areas and has implications in modelling other ecological processes.

Tree-ring parameters provide important information on tree growth variability and allow a retrospective analysis of tree growth responses to climate change, e.g. (Marchand et al., 2020; Spiecker, 2002). Data related to tree-ring patterns demonstrate varied growth patterns when exposed to water stress and before death (Barbeta & Penuelas, 2017). Isotopic information related

to tree rings also records the process of growth decline and eventually death due to carbon deprivation or nutrient deficiency related to long-term drought (Rodríguez-Calcerrada et al., 2017). The iWUE can be inferred through tree-ring $\delta^{13}C$, which simultaneously records the carbon assimilation and stomatal conductance, both of which are susceptible to environmental conditions (Timofeeva et al., 2017). Combined with stem growth information, iWUE and $\delta^{13}C$ are very useful for unraveling the hydraulic and carbon assimilation mechanisms underlying tree adaption to environmental stress (Bigler & Veblen, 2009; Levanič, Čater, & McDowell, 2011).

Poplar trees have been the preferred afforestation species to revitalize degraded land around the world based on their superior growth performance and adaptability to site conditions. Compared to natural forests, the planted forests are inherently lower in species richness and more uniform in stand structures (Li et al., 2009). Therefore, they seem to demonstrate varied response patterns to environmental stresses differently from natural forests (Brockerhoff, Jactel, Parrotta, Quine, & Sayer, 2008; Li et al., 2009). However, no definite conclusions have been reached as to whether plantations are more resistant to environmental stresses than natural forests or not. Such variances can be ascribed to climatic- or species-specific factors and management approaches, such as pruning and irrigation. Therefore, from both the socio-economic and ecological perspectives, an examination of growth and iWUE chronology of poplar plantations in cold semi-arid areas will provide information on growth response to climate change and C_a enrichment, and thus support the projection of future growth and the potential of this growth as a carbon sink for this ecosystem.

Emerging vegetation mortality has begun to impact the governmental policies (Allen et al., 2010; Dai, Trenberth, & Qian, 2004) due to its implications for ecosystem services and interactions between local mortality, carbon sinks and climate (Bertrand et al., 2011; Klein, Yakir, Buchmann,

& Grünzweig, 2014). Efforts to understand how rising C_a will interact with other environmental factors in determining the tree growth will contribute to understanding current forest decline and hence integrate forest management plans with different climatic scenarios. In this case, we focus on a better understanding of how plantation ecosystems adapt to warming and drying environments. The specific questions we address include: (1) how stem growth of different vigor classes is impacted by climatic factors and atmospheric C_a; and (2) to elucidate the mechanism underlying the forest decline from the perspective of carbon assimilation and water use strategy.

Methods and materials

Study area

The study area locates in Zhangbei county in Hebei Province, China (40°57'-41° 34' N ，114° 10'-115° 27' E, 1300 m-2128 m a.s.l). This area is under the control of the temperate continental climate. The precipitation is averaged at 392.7 mm. The precipitation majorly occurs during June and September which accounts for 64-69% of the annual total. The annual temperature is averaged at 4.1°C with a high diurnal-nocturnal temperature difference around 13~15°Cand the cumulative temperature is 2448°C. The frostless period adds up to 90~110 d. The area features strong wind with a wind gust of 10.8-13.8m/s amount to 50-70 days. Calcified layers are widely distributed in this area which may jeopardize the root absorption of water by the trees.

The shelterbelts are dominated by *Populus simonii* which are dated back to 1970s. All the sampled stands were planted by the year of 1975 and no forest management practice have been applied to them. The growth decline of poplar shelterbelts is characterized by severe defoliation and a high mortality rate. To compare poplar stands with varying symptoms of declination, we conducted a comprehensive field survey that included 27 sampling plots (Fig. S1) of three decline degrees

(Table 1) across the whole study area. At each site, we surveyed the tree height and DBH demography of each 20×20m plot. The health status of individual trees was assessed according to the crown defoliation rate. To avoid bias from the crown defoliation of similar sized-trees by different observers, we selected 6 individuals with the highest amount of leaves as a reference to 'healthy' trees. Declining trees were defined as individuals that showed dieback crown over 40%, and declining sites were defined as those contained over 20% dieback trees, among which a total of 20-60% dieback trees were classified as the first-degree decline (DI) stands and over 60% dieback trees as the second-degree decline (DII) stands (Table 1). The non-declining stands displayed a significantly lower ratio of dieback trees than that of the declining sites (4.8 ± 1.4% v.s. 22.7± 3.1%, Mann–Whitney test, $U = 6.9$, $P < 0.001$).

Insert Table 1

Environmental data

Monthly meteorological data (precipitation, temperature including the maximum, minimum and average values and relative humidity) of the study area from 1975 to 2016 were downloaded from the National Meteorological Science Data Center (http://data.cma.cn/). Kendall tests were conducted to confirm the data validity and representativeness of local climatic trends(Sun et al., 2018). Standardized Precipitation-Evapotranspiration Index (SPEI) was calculated using the SPEI (Standardized Precipitation Evapotranspiration Index) package in R (http://sac.csic.es/spei/) with a 12-month scale ($SPEI_{12}$) and was used to delineate the drought and non-drought periods. SPEI values above -0.5 represent no drought conditions (hereby indicated as S0), from -1.0 to –0.5 mild drought (SI), from -1.5 to -1.0 moderate drought (SII), from -2.0 to -1.5 severe drought (SIII), and

≤ -2.00 extreme drought (SIV) (Fig. 1). Ample evidence has shown stomatal sensitivity to high atmospheric demand driven by *VPD*. Consequently, *VPD* can pose drought-like water stress over plants, regardless of the soil water conditions. Therefore, we also calculated the *VPD* anomaly as the individual year's deviation from the mean of the entire study period (Fig. 1). The *VPD* was calculated as follows:

$$VPD = 0.611 \times \exp\left(17.502T/(T+240.97)\right) \times (1-RH) \qquad (1)$$

where T is temperature and RH is relative humidity.

Three soil columns were drilled from the surface to a depth of 400 cm at intervals of 20 cm in each plot. For each column, three replicates were performed at each depth. The samples of each layer were divided into three parts. One part of the 12 g soil samples at each layer was sealed in glass vials with Parafilm and frozen until isotopic analysis. The second part of the same depth was oven-dried at 105°C for 48 h to obtain the soil water content at the corresponding depths in each column. The average soil water at the same depth among all three columns was used to represent the soil water profile of the individual sites. The remaining soil samples were sent to the Beijing Agricultural and Forestry Academy lab to test the organic carbon, nitrogen, phosphorus, and potassium content (Fig. 1S).

Insert Fig. 1

Tree-ring sampling and measurements

We pooled 10 individuals for tree-ring examination in every sampling plot and retrieved two cores per tree perpendicularly at diameter at breast height (DBH, cm) with increment borers (Pressler 4.3mm). Finally, a total of 540 tree cores were obtained from the 27 plots of all three vigor

classes. The wood samples were dried at room temperature (°C) and polished with fine sandpapers. In brief, we measured the annual tree-ring widths to the nearest 0.01 mm with a stereomicroscope and the LINTAB system. The data were first processed with TSAP-Win V3.5(Rinntech, Hedelberg, Germany). Subsequently, COFECHA was used to validate the cross-dating of tree-ring measurements (Holmes, 1986). The chronologies of the trees from different vigor classes were determined using the ARSTAN program (Cook, 1985).

The age and radius expansion result in the gradual decreases of the ring width. However, increment in annual basal area (BAI, cm^2 $year^{-1}$) is less dependent on age and thus serves as an indicator of tree growth with the age effect eliminated (Battipaglia et al., 2013; Franco Biondi, 1999). It can increase accuracy in dendrochronological studies(Ding, Xiao, Tian, & Han, 2021) and climate response(Mohr, Saldana, Angulo, & Chhetri, 2019). Therefore, BAI is commonly used as a proxy for growth in ecology (Gómez−Guerrero et al., 2013; Silva & Anand, 2013). BAI was calculated as follows:

$$BAI = \pi\left(r_t^2 - r_{t-1}^2\right) \qquad (2)$$

where r_t and r_{t-1} represent the radius at the end and at the beginning of the annual tree-ring formation, respectively. Asymptotical BAI increases indicate tree growth in good condition(Franco Biondi & Qeadan, 2008), while decreasing BAI represents declining tree condition (Bigler & Bugmann, 2003, 2004; Wyckoff & Clark, 2000).

Tree ring chronology of carbon discrimination and iWUE

A scalpel was used to detach the individual rings of the cross-dated wood cores along ring lines under a stereomicroscope (40× magnification) and the rings of the same year were pooled to form

a composite sample (Liu et al., 2014; Wu et al., 2015) and represent the plot-aggregated isotopic composition changes. A strong correlation was found between the carbon sources of the whole wood and cellulose in terms of variation trends (Loader, Robertson, & McCarroll, 2003; Schleser & Jayasekera, 1985). Therefore, we used only whole wood for the $\delta^{13}C$ analysis as our objective was to trace the temporal tends and responses to climate variables rather than to recreate the historic climate (Sun et al., 2018). The composite wood samples were milled and then sieved through an 80-mesh sieve. One milligram wood powder was put into tin capsules for $\delta^{13}C$ analyses. $\delta^{13}C$ was determined by mass spectrometry (DELTA V Advantage; Thermo Scientific, Waltham, MA, USA; precision 0.1‰). Tree-ring $\delta^{13}C$ were corrected ($\delta^{13}C_{cor}$) to count for the Suess effect (McCarroll & Loader, 2004) according to the following equation:

$$\delta^{13}C_{cor}=\delta^{13}C_{tree}-(\delta^{13}C_a+6.4) \qquad (3)$$

where $\delta^{13}C_{tree}$ represents tree-ring $\delta^{13}C$, $\delta^{13}C_a$ is the atmospheric value. The Regional Curve Standardization method (RCS) were used to test and remove the age-related trend of $\delta^{13}C$ if proven to exist (e.g. (Esper, Cook, Krusic, Peters, & Schweingruber, 2003; Gagen, McCarroll, Robertson, Loader, & Jalkanen, 2008).

The preferential use of ^{12}C over ^{13}C during the process of photosynthesis gives rise to carbon isotopic discrimination ($\triangle$) between the plants and atmospheric CO_2. $\triangle$ is determined according to Farquhar and Richards (1984) as:

$$\Delta^{13}C=\frac{(\delta^{13}C_a-\delta^{13}C_{tree})}{(1+\delta^{13}C_{tree}/1000)} \qquad (4)$$

where $\delta^{13}C_a$ and $\delta^{13}C_{tree}$ represent the carbon isotope signatures of the air and the plant, respectively. $\triangle$ is also related to the ratio of intercellular (C_i) to atmospheric (C_a) CO_2 mole fraction, as follows:

$$\Delta^{13}C = \frac{a + (b - a)\ C_i}{C_a} \qquad (5)$$

where a is the constant fractionation during CO_2 diffusion through stomata (4.4‰) (O'Leary, 1981) and b is the biochemical fractionation during the Rubisco and PEP carboxylase reaction (≈27‰)(Farquhar & Richards, 1984). To support the calculation of Eq (4-5), the atmospheric CO_2 concentration and $\delta^{13}C_a$ values from 1977 to 2003 were obtained from a published study (McCarroll & Loader, 2004). For the period from 2004-2016, the measurements of C_a were retrieved from the Mauna Loa Observatory (http://cdiac.ornl.gov/trends/co_2/sio-mlo.html) and the $\delta^{13}C_a$ values were derived from ice cores.

iWUE (μmol mol^{-1}) was defined as the ratio of carbon assimilation to transpiration. This was calculated as follows:

$$iWUE = C_a(b - \triangle^{13}C)/(1.6(b-a)) \qquad (6)$$

Determination of current water source for different vigor classes

Ten individuals were randomly sampled from each stand. The isotopic campaigns were carried out twice every month between 08:30 and 11:00 a.m. from April to September in 2016.Three suberized branches were taken as xylem samples and sealed in the vials with Parafilm M® to avoid evaporation. The samples were immediately placed in a portable fridge box and stored in the lab fridge at -4°C until isotopic analysis.

Paired with xylem sampling, soil samples were collected simultaneously using ground augers and sealed as previously mentioned. A surface layer of approximately 3 cm of the soil sample was discarded to eliminate the possible evaporative enrichment effect of the uppermost layer. The soil samples were stored in a refrigerator until isotopic analysis.

Precipitation was sampled using three iron buckets in an open field. A tunnel with a table tennis ball at the collar was mounted on a bucket to reduce evaporative fractionation. The precipitation samples were collected after each rainfall event, sealed in polyethylene vials with Parafilm M® and transported back to the laboratory for refrigerated storage until analysis.

Water from xylem and soil samples was extracted by using the cryogenic vacuum distillation technique, and the isotopic compositions of the samples were measured with an analyzer of laser spectrometry for stable isotopes in liquid water (DLT-100, ABB Inc., USA) in the laboratory. The isotope ratios of $\delta^{18}O$ and δD were expressed as follows:

$$\delta^{18}O \text{ or } \delta D\ (‰) = (R_{sa}/R_{st} - 1) \times 1000 \quad (7)$$

where R_{sa} and R_{st} indicate the isotope ratios of the samples relative to the Vienna standard mean ocean water (VSMOW). The MixSIAR Bayesian mixing model was used to determine the contributions of potential water sources.

Data analysis

We used the Mann-Whitney U-test for non-parametric tests to compare the significant differences in dieback rates between the N and D stands. One-way ANOVA was used to test for significant differences in measurements among different vigor classes. We conducted Tukey's HSD test for post-hoc comparisons among groups. We adopted an analysis of covariance (ANCOVA) to test for differences in slope between two variables among vigor classes.

Inherent adaptive capacity in terms of carbon assimilation was interpreted based on the three theoretical scenarios(Saurer, Siegwolf, & Schweingruber, 2004): (1) c_i constant, (2) c_i/c_a constant, and (3) $c_a–c_i$ constant. The scenarios vary in the c_i changes with c_a, namely: (1) no c_i increase, (2) proportional c_i increases with c_a and (3) c_i increase rate same as c_a.

Correlation analysis has been widely used to analyze the influence of climatic variables on tree physiology (N. G. McDowell et al., 2010; Voltas et al., 2013). To examine the response of tree-ring growth to climate variables, Pearson's correlations were adopted to indicate the influence of precipitation, *VPD* and monthly temperature (T_{min}, T_{max} and $T_{average}$) on BAI. We conducted correlation assessment from previous July to the current September. A stepwise regression model was employed to identify the explanatory power of the climatic variables and air CO_2 over the tree ring growth.

Results

Long term growth and iWUE patterns of different vigor classes

Environmental statistics indicated an extremely low rainfall in 1997, amounting to only 245.2 mm. An increasing frequency of negative SPEI occurred afterwards (Fig. 1a). Similarly, no obvious trend was found for *VPD*, but the *VPD* anomaly exhibited increasing occurrences of higher *VPD* (compared with the average value during 1975-2016) since 1997 (Fig. 1b). When classified into contrasting SPEI and *VPD* ranges, BAI and iWUE exhibited significant differences among vigor classes (Table 2). The BAI of the N stands were always significantly higher than that of first-degree decline (DI), followed by second-degree decline (DII). However, this sequence was reversed in the comparison of iWUE of the three vigor classes. Moreover, the differences become increasingly significant between the two dieback classes during drought-stressed periods (SPEI≤-0.5 and *VPD*>0).

Insert Fig. 1

Insert Table 2

Trees in different vigor classes initially showed similar BAI but gradually shifted apart (Fig. 2a). Compared to the N stands, the significant differentiation of BAI towards lower values in DI and DII were dated in 1988 (p=0.02, one-way ANOVA) and 1985 (p=0.04, one-way ANOVA), respectively. Despite the varied BAI, trees of all vigor classes experienced continuous growth until around 2000. The maximum BAIs were pinpointed in 2003, 2002, and 1998 for the current N, DI, and DII classes, respectively. After reaching the growth climax, the BAI of all vigor classes demonstrated a noticeable decline. Over the whole study period, N stands were characterized by higher average BAI (mean ± SE=8.30 ± 0.58 cm^2 $year^{-1}$) than in DI (6.18 ± 0.42 cm^2 $year^{-1}$) and DII ones (4.11 ± 0.31 cm^2 $year^{-1}$).

Insert Fig. 2

All vigor classes exhibited increased iWUE from 1975 to 2016 (+37.7, +31.3, and +15.5 % for N, DI, and DII classes, respectively) (Fig. 2b). However, the stands of different health statuses displayed significant differences in the iWUE. DII stands presented the highest iWUE (mean ± SE =96.38 ± 1.51 μmol mol^{-1}), while N stands showed the lowest iWUE values (78.58 ± 0.60 μmol mol^{-1}) and DI stands displayed intermediate values (91.16 ± 1.21 μmol mol^{-1}; Fig. 3b).

Insert Fig. 3

Chronologies of $\delta^{13}C$, C_i and $\triangle^{13}C$

The original (Fig. 3) and the RCS $\delta^{13}C$ series (Fig. S2) do not show any increasing trend in the

young portion of the trees, indicating no juvenile effect of the carbon isotopic signature of trees in this area. After the Suess correction, tree-ring $\delta^{13}C$ series of the N stands still showed a marked decline (Fig. 3a). This decreasing trend of $\delta^{13}C$ became less significant as the health status of the trees deteriorated. DII barely showed any temporal trend in $\delta^{13}C$. The tree-rings recorded consistently higher $\delta^{13}C$ values of DII stands than the other two vigor classes, with the DI stands being the intermediate, and the N stands being the lowest (Fig. 3a; box plot). All stands displayed increased Ci along the progression of the year. However, the increasing trend became more plateau as the health status of the stands deteriorated. Except for the N stands, significant decreases in $\Delta^{13}C$ were observed over time for stands of both dieback degrees (Fig. 3c). Moreover, the decrease in slope became steeper as the tree health status deteriorated.

Relationship between historical tree growth and carbon use strategy of different vigor classes

The responses of BAI to iWUE, C_a, and $\delta^{13}C$ were demarcated by the year 2000, indicating that intense frequency of drought occurrence after 2000 had a great impact on the relationship between carbon use and growth trends for all health classes (Fig. 4). Since the initiation of 2000, stands of all health statuses showed a growth decline against increased iWUE (p=0.368, ANCOVA). However, compared to the steep decline of the current dieback stands, the N stands maintained growth by slowing down the decline (Fig. 4a). As for BAI response to C_a, all stands enhanced growth at increasing C_a before 2000 (p=0.405, ANCOVA), but this relationship declined afterwards (p=0.665, ANCOVA). $\delta^{13}C$ exhibited no significant influence on growth in all stands before 2000 (Fig. 4c). However, stands of different health statuses showed significantly different

growth responses to $\delta^{13}C$ afterwards ($p<0.01$, ANCOVA). The N stands enhanced their growth at increased $\delta^{13}C$ ($R^2=0.27$, $p<0.05$), while the dieback stands displayed a growth decline with increased $\delta^{13}C$ ($R^2=0.34$, $R^2=0.18$, for DI and DII, respectively, $p<0.05$).

Insert Fig. 4

Environmental drivers of the health status

The temporal trends of iWUE for N stands followed the predicted values in the scenario of constant C_i/C_a (Fig. 5a). In contrast, although mainly representing a constant C_i/C_a scenario, iWUE values of the D sites demonstrated a shifting tendency from the constant C_i/C_a scenario to the C_i constant scenario, which signified the independent response to C_a, especially after 1997 (Fig. 5b and c).

Insert Fig. 5

Trees of varied vigor classes exhibited different BAI responses to the monthly climate variables (Table 3). Compared with the D stands, the BAI of the N stands was more related to climate factors, especially temperature. The growing season temperature had a significant positive influence on the BAI of N and DI stands in both the previous and current years. In contrast, *VPD* and precipitation had little influence on tree growth. Obviously, the growth of the DII stands decoupled from climatic influences.

Insert Table 3

343 **Insert Table 4**

344

345 Stepwise regression analysis highlighted the triggering effect of growth decline due to the
346 sustained drought period (Table 4). The regression models captured the influence of climatic
347 variables on tree growth of all vigor classes (R^2>0.8) in the period before 2000 and R^2>0.6, in the
348 period after 2000 when C_a was included. The BAI of all vigor classes showed positive responses
349 to historical CO_2 but changed to negative responses after 2000. In contrast, the sole explanatory
350 power of cumulative annual temperature and SPEI on BAI was limited and failed to count the BAI
351 variances of DII stands.

352

353 **Variances of soil water and nutrition acquisition of different vigor classes**

354 The comparison of on-site soil water and nutritional sources revealed significant differences
355 among stands of contrasting health status (Fig. 6 and 7). The stand soil moisture of different vigor
356 classes was close at the layers above 100 cm but differentiated notably with depth. In particular,
357 the healthy and DI stands had a much higher soil moisture below 200 cm than the DII stands
358 (p=0.018, one-way ANOVA). Below 250 cm, the soil water of the DI stands began to decrease
359 significantly compared to that of the healthy stands (p<0.001, one-way ANOVA). The N stands
360 showed significantly higher available nitrogen in all soil layers than the dieback counterparts (Fig.
361 6b). A significant difference in available nitrogen was found between the two declined classes
362 only in the surface layer of 0-40 cm.

363 Isotope analysis of water source contribution showed contrasting water uptake distributions
364 among stands of different health statuses (Fig. 7). N stands preferred water from deeper layers
365 (lower than 160 cm). In contrast, the DI stands mainly obtained water from the middle layers of

120-160 cm, and water from relatively shallow layers of 0-120 cm constituted the major water sources for the DII stands. Clearly, stands of unfavorable health conditions shifted the depth of water absorption.

Insert Fig. 6

Insert Fig. 7

Discussion

4.1 Varied ability to access the deep soil water modulating the growth response of different vigor classes to climatic influences

Analyzing the growth-climate relationships may provide us with a perspective in understanding the varied relationship between iWUE and growth enhancement. A remarkable outcome of this study is that tree growth increasing decoupled with climatic factors as the health status deteriorated. We found a significant correlation between the growth of healthy stands and growing season temperatures in previous and current years. In contrast, DII stands exhibited no response to climatic influences. Insignificant or negative relationships between iWUE and stem growth are commonly attributed to the predominant influence of stress (Lévesque, Siegwolf, Saurer, Eilmann, & Rigling, 2014; Liu et al., 2014). However, we found that precipitation and *VPD* exerted almost no significant influence on stem growth for all vigor classes, implying a reliance on other water sources in this area. Ground water has been suggested as an important water source for trees in this area (Sun et al., 2018). Although groundwater samples were not obtained, our isotopic observation of the water use profile showed a clear pattern of accessing deep layer soil water as the health status of stands improved. Therefore, soil water supply buffered the health of trees from

the influence of precipitation and *VPD* fluctuations, which have been regarded as the drivers of tree decline (Eamus, Boulain, Cleverly, & Breshears, 2013).

As the increase in temperature would benefit tree growth by prolonging the growing season, access to the deep soil water might also contribute to the positive effects of air temperature on stem growth in the normal stands. Earlywood formation, which occurs at the beginning of the growing season, requires carbohydrates stored during the previous growing season (Litton, Raich, & Ryan, 2007). Therefore, a warmer climate with reduced water stress by the end of the growing season would result in carbon storage for the following growing season. The effect of deep water supply in ameliorating drought stress on stem growth is consistent with that found in British Columbia (Cortini et al., 2011) the northern Rocky Mountains (Reed et al., 2018), and Albeta (Chhin, Hogg, Lieffers, & Huang, 2008). However, the existence of calcified soil layers in declined stands constrains the root accessibility to deep-layer water. The cumulative effect of chronic water shortage would cause the loss of xylem hydraulic function and thus vitality decrease in response to climatic influences.

4.2 Physiological mechanism underlying the health status of trees

We found that iWUE at DI and DII responses to atmospheric C_a increases shift from independent from C_a (C_i constant) to active (C_i/C_a constant). These results indicate that trees in this area might adopt dynamic leaf gas exchange strategies, which are derived from different environmental factors, with respect to elevating C_a (Voelker et al., 2016).

Physiological variability (i.e. iWUE, $\triangle^{13}C$) translated to variability in growth. In our study, the iWUE trend of the declined stands gradually shift from the 'C_i/C_a scenario' toward 'constant C_i scenario'. In both scenarios, the iWUE in our study area indicates the constrained stomatal

412 conductance as a result of the rising c_a, or an increased photosynthesis rate (A) with constant g_s
413 (Kwak et al., 2016). However, the switch between scenarios indicated a higher sensitivity of
414 declined stands to C_a than the healthy ones. The increased physiological sensitivity has further
415 implications on growth rate, as we found a higher explanatory power of C_a on BAI (Table 4) in
416 declined stands. Secondary growth can serve as a proxy of net carbon gain(Voltas et al., 2013),
417 therefore, the trend of increasing iWUE along with decreasing growth suggests a reduction in
418 water loss, either through decreased water absorption or stomatal conductance, rather than an
419 increase in assimilation over time. This agrees with the results of previous studies (Linares,
420 Delgado-Huertas, Camarero, Merino, & Carreira, 2009; Maseyk, Hemming, Angert, Leavitt, &
421 Yakir, 2011; Voltas et al., 2013). In our study, this realization can be substantiated by the varied
422 ability to access deep soil water across the vigor classes. Exposed to long-term water limitation,
423 trees will adopt strict stomatal regulation to maintain the xylem hydraulic function or the stomatal
424 closure prevails due to the loss of hydraulic conductance. In either case, water loss from
425 transpiration would be greatly reduced, contributing to increased iWUE in all stands. As the water
426 became more stressed under more declined stands, the stomatal closure became more severe and
427 led to a steep increase in the iWUE trend.
428 Stomatal control also leads to iWUE variation by regulation of the photosynthetic process which is
429 also partially influenced by factors such as C_a (Ainsworth & Long, 2005; Tricker et al., 2005) and
430 climate (Fernández-de-Uña et al., 2016). C_a elevation leads to a decrease in stomatal conductance
431 and an increase in photosynthetic assimilation, both of which induce greater iWUE (Battipaglia et
432 al., 2013). Therefore, compared with the declined stands, the long-term gentle increase of iWUE
433 in the healthy stands, indicating weak stimulation of photosynthesis under increasing CO_2. This is

either because of the constraint on photosynthesis from environmental factors other than CO_2 or a less pronounced stomatal conductance decrease under weaker water limitation. In declined stands, our observations complied with the fact that trees downscaled stomatal conductance under water stress to minimize water loss through transpiration, and thus lead to increased ^{13}C in plant biomass and decreased $\Delta^{13}C$ (Scheidegger, Saurer, Bahn, & Siegwolf, 2000). Moreover, as the changing direction (increasing or decreasing) of C_i indicates stomatal closure, the decreasing C_i as the stand health status deteriorates also indicates stricter stomatal control in declined stands than in their healthy counterparts. Severe stomatal closure may lead to higher leaf temperatures and, thus, increased respiratory carbon loss (Körner, 2006). Therefore, even without the measurement of ^{18}O in tree rings, our results support the idea that reduction of stomatal conductance might pose strong limitations on carbon absorption in trees in our declined stands regardless of increasing C_a. The stomatal closure of the declined trees where soil water stress was intense can also explain the divergent isotope response and growth to climatic factors among stands of different health status. This further supports the role of local soil water conditions in determining the physiological responses of trees to climate warming and changing C_a, and also explained our differences with other studies where declined trees showed greater sensitivity to climatic factors (Macalady & Bugmann, 2014; N. G. McDowell et al., 2010).

4.3 Increases in iWUE do not necessarily covert to growth enhancement

We found a decoupling between stem growth and iWUE over a 15-year period of continuous drought stress (Fig. 3 and Fig. 4a). Similar growth declines accompanied by an increase in iWUE have also been reported in various ecosystems, including arid and semiarid forests in the

456 Mediterranean (Lévesque et al., 2014), northwestern China (Wu et al., 2015) and tropical
457 regions(van der Sleen et al., 2015). Such decoupling between iWUE and BAI indicates that the
458 increase in iWUE did not necessarily promote plant growth, and other factors might offset the
459 stimulating effect of CO_2 on growth.
460 The declining stem growth trends during the recent decade of the study period could be partially
461 attributed to the aging effect. *Populus simonii* generally steps into stem growth slowdown around
462 20 years of age and experiences low annual increments afterwards (Tang & Zhang, 2000). The
463 trees in our study were 40 years old. Therefore, the lack of iWUE stimulation on stem growth
464 could be ascribed to the aging process. However, iWUE in the DII stands is constantly higher than
465 the health stands, indicating that the decoupling between iWUE and BAI is also the result of
466 additional factors other than age.
467 Compared with healthy trees, the declined trees can present either higher BAI with lower iWUE
468 (Voltas et al., 2013; Zadworny et al., 2019) or lower BAI with higher iWUE (Timofeeva et al.,
469 2017). The first condition can be explained by the cavitation-susceptible xylem conduits because
470 of fast growth or unsustainable growth support from low-rate carbon assimilation and other
471 nutrients (Zadworny et al., 2019). The second condition is mainly caused by water limitations and
472 depends on different environmental influences (Hereş, Voltas, López, & Martínez-Vilalta, 2014;
473 N. G. McDowell et al., 2010). At first glance, the effect of precipitation on radial growth in our
474 case was rather weak (Table 3). However, we observed a downward migration of water absorption
475 depths as the stands' health status improved, implying the dominant role of the soil water supply
476 from deep layers over precipitation in supporting transpiration in our study area. Therefore, the
477 inaccessibility of deep water posed water stress for trees and was responsible for the declination of

stands (DI and DII stand). This conclusion has also been upheld by Sun *et al*., 2018 who found the dominant role of groundwater depth on iWUE over other climatic factors in similar areas. In our case, the contrasting water availability renders trees to face water deficiency of different severities over time. The more stressed trees experience long-term severe stomatal control to preserve their xylem hydraulic function at the expense of carbon assimilation. This strategy increases iWUE but leads to low stem growth. As a result, trees demonstrate growth deviation from a very early age. The differentiation of the growth status would further exacerbate by triggering events, such as extremely low supplementation from rainfall and consecutive drought years, such as in 1997 and continuous dry years in our study. Extreme summer drought has been proven to be responsible for causing hydraulic failure, dieback, and mortality (Nardini et al., 2016). The timing and severity of drought add up to the complexity of "legacy effects" on tree stem radial growth and reduce the resilience of trees (Gao et al., 2018). For example, the carbon sequestration rate in drought-prone forests may not increase with elevated C_a levels, as predicted by the models and controlled experiments (Nowak, Ellsworth, & Smith, 2004; Sitch et al., 2008). Our evidence of the predominant role of water stress over other stimulating factors on tree growth reinforces the point that stand-level water limitation may constrain the adaptability of forests to climatic warming in drought-sensitive areas.

Beside of the soil water, we found significantly lower soil nitrogen content across stands with varying health status. It has been shown that nutrient availability, particularly nitrogen, limits forest growth under elevated CO_2 conditions (Fisher, Badgley, & Blyth, 2012). Even without tree ring ^{15}N to clarify whether site-specific nutrient availability was limited, our results also indicate nutrient factors in explaining growth decline, and thus the deviation of growth trend from iWUE.

Conclusions

Our study shows that the boosting effect that may have been generated by CO_2 elevation, rising temperatures, or their synergies on stem growth in the semi-arid cold area, cannot offset the existence of soil moisture stress, especially after a series of droughts. Based on the trend of iWUE and ^{13}C and the soil water absorption profile, we believe that trees facing chronic soil water stress would prevent excessive water loss through stomatal control, leading to rising iWUE. Meanwhile, an increase *in* C_i indicates no apparent limitation on CO_2 absorption. This is a direct embodiment of the boosting effect of rising C_a concentrations on iWUE. However, the boosting effect cannot offset the cumulative soil water stress on growth. High iWUE does not translate to growth or increased vigor of trees, especially after a drought series. Compared with precipitation, access of deep soil water is associated with health status, implying its importance as the main water resource of poplar plantations in this area. Therefore, we suggest that soil moisture conditions the iWUE and growth sensitivity to global warming and thus portray site-specific decline episodes of different degrees in drought-prone areas.

Acknowledgement

The co-authors have no conflict of interest to declare. We greatly appreciate the financial supports from the Fundamental Research Funds for the Central Universities (2019ZY35) and the National Science Foundation in China (41977149 and 41877152).

References

Ainsworth, E. A., & Long, S. P. (2005). What have we learned from 15 years of free-air CO_2 enrichment (FACE)? A meta-analytic review of the responses of photosynthesis, canopy properties and plant production to rising CO_2. *New Phytologist, 165*(2), 351-372.

Allen, C. D., & Breshears, D. D. (1998). Drought-induced shift of a forest–woodland ecotone: rapid landscape response to climate variation. *Proceedings of the National Academy of Sciences, 95*(25), 14839-14842.

Allen, C. D., Breshears, D. D., & McDowell, N. G. (2015). On underestimation of global vulnerability to tree mortality and forest die-off from hotter drought in the Anthropocene. *Ecosphere, 6*(8), 1-55.

Allen, C. D., Macalady, A. K., Chenchouni, H., Bachelet, D., McDowell, N., Vennetier, M., . . . Hogg, E. T. (2010). A global overview of drought and heat-induced tree mortality reveals emerging climate change risks for forests. *Forest ecology & management, 259*(4), 660-684.

Barbeta, A., & Penuelas, J. J. G. c. b. (2017). Increasing carbon discrimination rates and depth of water uptake favor the growth of Mediterranean evergreen trees in the ecotone with temperate deciduous forests. *Global Change Biology, 23*(12), 5054-5068.

Battipaglia, G., Saurer, M., Cherubini, P., Calfapietra, C., McCarthy, H. R., Norby, R. J., & Francesca Cotrufo, M. (2013). Elevated CO_2 increases tree-level intrinsic water use efficiency: Insights from carbon and oxygen isotope analyses in tree rings across three forest FACE sites. *New Phytologist, 197*(2), 544-554.

Bertrand, R., Lenoir, J., Piedallu, C., Riofrio-Dillon, G., de Ruffray, P., Vidal, C., Gégout, J.-C. (2011). Changes in plant community composition lag behind climate warming in lowland forests. *Nature, 479*(7374), 517-520.

Bigler, C., & Bugmann, H. (2003). Growth-dependent tree mortality models based on tree rings. *Canadian Journal of Forest Research, 33*(2), 210-221.

Bigler, C., & Bugmann, H. (2004). Predicting the time of tree death using dendrochronological data. *Ecological Applications, 14*(3), 902-914.

Bigler, C., & Veblen, T. T. (2009). Increased early growth rates decrease longevities of conifers in subalpine forests. *Oikos, 118*(8), 1130-1138.

Biondi, F. (1999). Comparing tree-ring chronologies and repeated timber inventories as forest monitoring tools. *Ecological Applications, 9*(1), 216-227.

Biondi, F., & Qeadan, F. (2008). A theory-driven approach to tree-ring standardization: defining the biological trend from expected basal area increment. *Tree-Ring Research, 64*(2), 81-96.

Breshears, D. D., & Allen, C. D. (2002). The importance of rapid, disturbance-induced losses in carbon management and sequestration. *Global Ecology & Biogeography, 11*(1), 1-5.

Breshears, D. D., Cobb, N. S., Rich, P. M., Price, K. P., Allen, C. D., Balice, R. G., Belnap, J. (2005). Regional vegetation die-off in response to global-change-type drought. *Proceedings of the National Academy of Sciences, 102*(42), 15144-15148.

Brockerhoff, E. G., Jactel, H., Parrotta, J. A., Quine, C. P., & Sayer, J. (2008). Plantation forests and biodiversity: oxymoron or opportunity? *Biodiversity Conservation, 17*(5),

925-951.
Chhin, S., Hogg, E. T., Lieffers, V. J., & Huang, S. (2008). Potential effects of climate change on the growth of lodgepole pine across diameter size classes and ecological regions. *Forest ecology & management, 256*(10), 1692-1703.
Cortini, F., Comeau, P. G., Boateng, J. O., Bedford, L., McClarnon, J., & Powelson, A. (2011). Effects of climate on growth of lodgepole pine and white spruce following site preparation and its implications in a changing climate. *Canadian Journal of Forest Research, 41*(1), 180-194.
Dai, A., Trenberth, K. E., & Qian, T. (2004). A global dataset of Palmer Drought Severity Index for 1870–2002: Relationship with soil moisture and effects of surface warming. *Journal of Hydrometeorology, 5*(6), 1117-1130.
Dietrich, R., Bell, F. W., Silva, L. C., Cecile, A., Horwath, W. R., & Anand, M. (2016). Climatic sensitivity, water-use efficiency, and growth decline in boreal jack pine (*Pinus banksiana*) forests in Northern Ontario. *Journal of Geophysical Research: Biogeosciences, 121*(10), 2761-2774.
Ding, A.-J., Xiao, S.-C., Tian, Q.-Y., & Han, C. (2021). Correcting Eccentric Growth Rings Using Basal Area Increment: A Case Study for a Desert Shrub in Northwestern China. *Tree-Ring Research, 77*(1), 1-9.
Eamus, D., Boulain, N., Cleverly, J., & Breshears, D. D. (2013). Global change-type drought-induced tree mortality: vapor pressure deficit is more important than temperature per se in causing decline in tree health. *Ecology & Evolution, 3*(8), 2711-2729.
Esper, J., Cook, E. R., Krusic, P. J., Peters, K., & Schweingruber, F. H. (2003). Tests of the RCS method for preserving low-frequency variability in long tree-ring chronologies. *Tree-Ring Research, 59*(2), 81-98.
Farquhar, G., & Richards, R. (1984). Isotopic composition of plant carbon correlates with water-use efficiency of wheat genotypes. *Functional Plant Biology, 11*(6), 539-552.
Fernández-de-Uña, L., McDowell, N. G., Cañellas, I., & Gea-Izquierdo, G. (2016). Disentangling the effect of competition, CO_2 and climate on intrinsic water-use efficiency and tree growth. *Journal of Ecology, 104*(3), 678-690.
Fisher, J. B., Badgley, G., & Blyth, E. (2012). Global nutrient limitation in terrestrial vegetation. *Global Biogeochemical Cycles, 26*(3).
Fu, C. (2007). Evidences of drying trend in the global during the later half of 20th century and their relationship with large-scale climate background. *Science in China Series D-Earth Sciences, 50*(5), 776-788.
Gagen, M., McCarroll, D., Robertson, I., Loader, N. J., & Jalkanen, R. (2008). Do tree ring δ13C series from Pinus sylvestris in northern Fennoscandia contain long-term non-climatic trends? *Chemical Geology, 252*(1-2), 42-51.
Gao, S., Liu, R., Zhou, T., Fang, W., Yi, C., Lu, R., Luo, H. (2018). Dynamic responses of tree-ring growth to multiple dimensions of drought. *Global Change Biology, 24*(11), 5380-5390.
Gómez-Guerrero, A., Silva, L. C., Barrera-Reyes, M., Kishchuk, B., Velázquez-Martínez, A., Martínez-Trinidad, T., . . . Horwath, W. R. (2013). Growth decline and divergent tree ring isotopic composition ($\delta^{13}C$ and $\delta^{18}O$) contradict predictions of CO_2 stimulation in high altitudinal forests. *Global Change Biology, 19*(6), 1748-1758.

611 Hereș, A.-M., Voltas, J., López, B. C., & Martínez-Vilalta, J. (2014). Drought-induced mortality
612 selectively affects Scots pine trees that show limited intrinsic water-use efficiency
613 responsiveness to raising atmospheric CO2. *Functional Plant Biology, 41*(3), 244-
614 256.
615 Huang, J.-p., Guan, X.-d., & Ji, F. (2012). Enhanced cold-season warming in semi-arid
616 regions. *Atmospheric Chemistry & Physics, 12*(12), 5391-5398.
617 Klein, T., Yakir, D., Buchmann, N., & Grünzweig, J. M. (2014). Towards an advanced
618 assessment of the hydrological vulnerability of forests to climate change-induced
619 drought. *New Phytologist, 201*(3), 712-716.
620 Körner, C. (2006). Plant CO_2 responses: an issue of definition, time and resource supply. *New*
621 *Phytologist, 172*(3), 393-411.
622 Kurz, W. A., Dymond, C., Stinson, G., Rampley, G., Neilson, E., Carroll, A., Safranyik, L.
623 (2008). Mountain pine beetle and forest carbon feedback to climate change. *Nature,*
624 *452*(7190), 987-990.
625 Kwak, J.-H., Lim, S.-S., Lee, K.-S., Viet, H. D., Matsushima, M., Lee, K.-H., Chang, S. X.
626 (2016). Temperature and air pollution affected tree ring δ13C and water-use
627 efficiency of pine and oak trees under rising CO2 in a humid temperate forest.
628 *Chemical Geology, 420*, 127-138.
629 Levanič, T., Čater, M., & McDowell, N. G. (2011). Associations between growth, wood
630 anatomy, carbon isotope discrimination and mortality in a Quercus robur forest. *Tree*
631 *physiology, 31*(3), 298-308.
632 Lévesque, M., Siegwolf, R., Saurer, M., Eilmann, B., & Rigling, A. (2014). Increased water-
633 use efficiency does not lead to enhanced tree growth under xeric and mesic
634 conditions. *New Phytologist, 203*(1), 94-109.
635 Li, S., Luo, Y.-q., Wu, J., Zong, S.-x., Yao, G.-l., Li, Y., Zhang, Y.-r. (2009). Community
636 structure and biodiversity in plantations and natural forests of seabuckthorn in
637 southern Ningxia, China. *Forestry Studies in China, 11*(1), 49-54.
638 Linares, J.-C., Delgado-Huertas, A., Camarero, J. J., Merino, J., & Carreira, J. A. (2009).
639 Competition and drought limit the response of water-use efficiency to rising
640 atmospheric carbon dioxide in the Mediterranean fir Abies pinsapo. *Oecologia,*
641 *161*(3), 611-624.
642 Litton, C. M., Raich, J. W., & Ryan, M. G. (2007). Carbon allocation in forest ecosystems.
643 *Global Change Biology, 13*(10), 2089-2109.
644 Liu, X., Wang, W., Xu, G., Zeng, X., Wu, G., Zhang, X., & Qin, D. (2014). Tree growth and
645 intrinsic water-use efficiency of inland riparian forests in northwestern China:
646 evaluation via δ13C and δ18O analysis of tree rings. *Tree physiology, 34*(9), 966-980.
647 Loader, N., Robertson, I., & McCarroll, D. (2003). Comparison of stable carbon isotope ratios
648 in the whole wood, cellulose and lignin of oak tree-rings. *Palaeogeography,*
649 *Palaeoclimatology, Palaeoecology, 196*(3-4), 395-407.
650 Macalady, A. K., & Bugmann, H. (2014). Growth-mortality relationships in piñon pine (*Pinus*
651 *edulis*) during severe droughts of the past century: shifting processes in space and
652 time. *PloS one, 9*(5), e92770.
653 Marchand, W., Girardin, M. P., Hartmann, H., Depardieu, C., Isabel, N., Gauthier, S.,
654 Bergeron, Y. (2020). Strong overestimation of water-use efficiency responses to

rising CO_2 in tree-ring studies. *Global Change Biology, 26*(8), 4538-4558.
Maseyk, K., Hemming, D., Angert, A., Leavitt, S. W., & Yakir, D. (2011). Increase in water-use efficiency and underlying processes in pine forests across a precipitation gradient in the dry Mediterranean region over the past 30 years. *Oecologia, 167*(2), 573-585.
McCarroll, D., & Loader, N. J. (2004). Stable isotopes in tree rings. *Quaternary Science Reviews, 23*(7-8), 771-801.
McDowell, N., Pockman, W. T., Allen, C. D., Breshears, D. D., Cobb, N., Kolb, T., Williams, D. G. (2008). Mechanisms of plant survival and mortality during drought: why do some plants survive while others succumb to drought? *New Phytologist, 178*(4), 719-739.
McDowell, N. G., Allen, C. D., & Marshall, L. (2010). Growth, carbon-isotope discrimination, and drought-associated mortality across a Pinus ponderosa elevational transect. *Global Change Biology, 16*(1), 399-415.
Mohr, M. D., Saldana, D., Angulo, G. S., & Chetri, P. K. (2019). *Tree-ring growth response of Jeffrey Pine to climate in northern California.* Paper presented at the AGU Fall Meeting Abstracts.
Nardini, A., Casolo, V., Dal Borgo, A., Savi, T., Stenni, B., Bertoncin, P., McDowell, N. G. (2016). Rooting depth, water relations and non-structural carbohydrate dynamics in three woody angiosperms differentially affected by an extreme summer drought. *Plant, Cell and Environment, 39*(3), 618-627.
Newman, B. D., Wilcox, B. P., Archer, S. R., Breshears, D. D., Dahm, C. N., Duffy, C. J., Vivoni, E. R. (2006). Ecohydrology of water-limited environments: A scientific vision. *Water resources research, 42*(6).
Norby, R. J., DeLucia, E. H., Gielen, B., Calfapietra, C., Giardina, C. P., King, J. S., Ceulemans, R. (2005). Forest response to elevated CO_2 is conserved across a broad range of productivity. *Proceedings of the National Academy of Sciences, 102*(50), 18052-18056.
Nowak, R. S., Ellsworth, D. S., & Smith, S. D. (2004). Functional responses of plants to elevated atmospheric CO_2–do photosynthetic and productivity data from FACE experiments support early predictions? *New Phytologist, 162*(2), 253-280.
O'Leary, M. H. (1981). Carbon isotope fractionation in plants. *Phytochemistry, 20*(4), 553-567.
Peñuelas, J., Canadell, J. G., & Ogaya, R. (2011). Increased water-use efficiency during the 20th century did not translate into enhanced tree growth. *Global Ecology Biogeography, 20*(4), 597-608.
Raffa, K. F., Aukema, B. H., Bentz, B. J., Carroll, A. L., Hicke, J. A., Turner, M. G., & Romme, W. H. (2008). Cross-scale drivers of natural disturbances prone to anthropogenic amplification: the dynamics of bark beetle eruptions. *Bioscience, 58*(6), 501-517.
Reed, C. C., Ballantyne, A. P., Cooper, L. A., & Sala, A. (2018). Limited evidence for CO_2-related growth enhancement in northern Rocky Mountain lodgepole pine populations across climate gradients. *Global Change Biology, 24*(9), 3922-3937.
Rodríguez-Calcerrada, J., Sancho-Knapik, D., Martin-StPaul, N. K., Limousin, J.-M., McDowell, N. G., & Gil-Pelegrín, E. (2017). Drought-induced oak decline—factors involved, physiological dysfunctions, and potential attenuation by forestry practices. In *Oaks Physiological Ecology. Exploring the Functional Diversity of Genus Quercus L.* (pp. 419-451): Springer.

Rotenberg, E., & Yakir, D. (2010). Contribution of semi-arid forests to the climate system. *Science, 327*(5964), 451-454.

Saurer, M., Siegwolf, R. T., & Schweingruber, F. H. (2004). Carbon isotope discrimination indicates improving water-use efficiency of trees in northern Eurasia over the last 100 years. *Global Change Biology, 10*(12), 2109-2120.

Scheidegger, Y., Saurer, M., Bahn, M., & Siegwolf, R. (2000). Linking stable oxygen and carbon isotopes with stomatal conductance and photosynthetic capacity: a conceptual model. *Oecologia, 125*(3), 350-357.

Schleser, G., & Jayasekera, R. (1985). δ 13 C-variations of leaves in forests as an indication of reassimilated CO_2 from the soil. *Oecologia, 65*(4), 536-542.

Shen, X., Liu, B., Xue, Z., Jiang, M., Lu, X., & Zhang, Q. (2019). Spatiotemporal variation in vegetation spring phenology and its response to climate change in freshwater marshes of Northeast China. *Science of the Total Environment, 666*, 1169-1177.

Silva, L. C., & Anand, M. (2013). Probing for the influence of atmospheric CO2 and climate change on forest ecosystems across biomes. *Global Ecology & Biogeography, 22*(1), 83-92.

Silva, L. C., Anand, M., & Leithead, M. D. J. P. o. (2010). Recent widespread tree growth decline despite increasing atmospheric CO_2. *PloS one, 5*(7), e11543.

Sitch, S., Huntingford, C., Gedney, N., Levy, P., Lomas, M., Piao, S., Friedlingstein, P. (2008). Evaluation of the terrestrial carbon cycle, future plant geography and climate-carbon cycle feedbacks using five Dynamic Global Vegetation Models (DGVMs). *Global Change Biology, 14*(9), 2015-2039.

Spiecker, H. (2002). Tree rings and forest management in Europe. *Dendrochronologia, 20*(1-2), 191-202.

Suarez, M. L., Ghermandi, L., & Kitzberger, T. (2004). Factors predisposing episodic drought-induced tree mortality in Nothofagus–site, climatic sensitivity and growth trends. *Journal of Ecology, 92*(6), 954-966.

Sun, S., He, C., Qiu, L., Li, C., Zhang, J., & Meng, P. (2018). Stable isotope analysis reveals prolonged drought stress in poplar plantation mortality of the Three-North Shelter Forest in Northern China. *Agricultural & Forest Meteorology, 252*, 39-48.

Tang, R., & Zhang, Y. (2000). The Growing Regularity of *Populus simonii* in Gully Rolling Region of Shaanxi Loess Plateau. *Journal of Northwest Forestry University, 15*, 15-19.

Timofeeva, G., Treydte, K., Bugmann, H., Rigling, A., Schaub, M., Siegwolf, R., & Saurer, M. (2017). Long-term effects of drought on tree-ring growth and carbon isotope variability in Scots pine in a dry environment. *Tree physiology, 37*(8), 1028-1041.

Tricker, P. J., Trewin, H., Kull, O., Clarkson, G. J., Eensalu, E., Tallis, M. J., Taylor, G. (2005). Stomatal conductance and not stomatal density determines the long-term reduction in leaf transpiration of poplar in elevated CO_2. *Oecologia, 143*(4), 652-660.

van der Sleen, P., Groenendijk, P., Vlam, M., Anten, N. P. R., Boom, A., Bongers, F., Zuidema, P. A. (2015). No growth stimulation of tropical trees by 150 years of CO_2 fertilization but water-use efficiency increased. *Nature Geoscience, 8*(1), 24-28. doi:10.1038/ngeo2313

Van Mantgem, P. J., Stephenson, N. L., Byrne, J. C., Daniels, L. D., Franklin, J. F., Fulé, P.

Z., Taylor, A. H. (2009). Widespread increase of tree mortality rates in the western United States. *Science, 323*(5913), 521-524.

Voelker, S. L., Brooks, J. R., Meinzer, F. C., Anderson, R., Bader, M. K. F., Battipaglia, G., Betancourt, J. L. (2016). A dynamic leaf gas-exchange strategy is conserved in woody plants under changing ambient CO_2: evidence from carbon isotope discrimination in paleo and CO_2 enrichment studies. *Global Change Biology, 22*(2), 889-902.

Voltas, J., Camarero, J. J., Carulla, D., Aguilera, M., Ortiz, A., & Ferrio, J. P. J. P., Cell. (2013). A retrospective, dual-isotope approach reveals individual predispositions to winter-drought induced tree dieback in the southernmost distribution limit of Scots pine. *Plant, Cell & Environment, 36*(8), 1435-1448.

Wei, P., Xu, L., Pan, X., Hu, Q., Li, Q., Zhang, X., Wang, X. (2020). Spatio-temporal variations in vegetation types based on a climatic grassland classification system during the past 30 years in Inner Mongolia, China. *Catena, 185*, 104298.

Williams, A. P., Allen, C. D., Macalady, A. K., Griffin, D., Woodhouse, C. A., Meko, D. M., Grissino-Mayer, H. D. (2013). Temperature as a potent driver of regional forest drought stress and tree mortality. *Nature climate change, 3*(3), 292-297.

Wu, G., Liu, X., Chen, T., Xu, G., Wang, W., Zeng, X., & Zhang, X. (2015). Elevation-dependent variations of tree growth and intrinsic water-use efficiency in Schrenk spruce (*Picea schrenkiana*) in the western Tianshan Mountains, China. *Frontiers in Plant Science, 6*, 309.

Wyckoff, P. H., & Clark, J. S. (2000). Predicting tree mortality from diameter growth: a comparison of maximum likelihood and Bayesian approaches. *Canadian Journal of Forest Research, 30*(1), 156-167.

Zadworny, M., Jagodziński, A. M., Łakomy, P., Mucha, J., Oleksyn, J., Rodríguez-Calcerrada, J., & Ufnalski, K. (2019). Regeneration origin affects radial growth patterns preceding oak decline and death–insights from tree-ring $\delta^{13}C$ and $\delta^{18}O$. *Agricultural & Forest Meteorology, 278*, 107685.

773 **Tables**

774 **Table 1** Summary of sampling plots of different vigor classes.

775 **Table 2** Comparison of the BAI (cm^2 $year^{-1}$) and iWUE (μmol mol^{-1}) among stands of different

776 health status in contrasting SPEI and VPD conditions. Values are given as mean ± S.D.

777 **Table 3** Relationship between tree growth and monthly climatic variables.

778 **Table 4** Coefficients of predictors from the stepwise regression analysis summary over the

779 relationship between BAI and climatic variables (precipitation, *VPD*, c_a and T_c) in all vigor classes.

780

781

782 Table 1 Summary of sampling plots of different vigor classes

Vigor classes	Height (m)	DBH (cm)	Sites (subplots)	Altitude range (m)	Density (ha^{-1})	Rate of dieback trees (%)
N	13.88±4.25	22.15±2.25	9(3)	1250-1275	950-1005	0
DI	10.82±2.25	17.62±1.86	9(3)	1238-1285	946-998	20-60
DII	8.95±2.25	13.71±1.64	9(3)	1256-1286	982-1012	>60

783 Abbreviations: N for normal stands; DI for stands of Dieback I degree; DII for stands of Dieback

784 II degree

785

Table 2 Comparison of the BAI (cm^2 $year^{-1}$) and iWUE (μmol mol^{-1}) among stands of different health status in contrasting SPEI and VPD conditions. Values are given as mean ± S.D.

Periods	BAI			iWUE		
	N	DI	DII	N	DI	DII
Annual SPEI>-0.5	7.63±3.58[a]	5.93±5.93[b]	4.17±4.17[b]	77.60±3.92[a]	90.713±8.25[b]	95.78±10.21[c]
Annual SPEI≤-0.5	8.83±4.14[a]	6.25±2.71[b]	3.78±1.85[c]	80.65±8.94[a]	92.61±6.25[b]	98.33±3.78[c]
Growing season SPEI>-0.5	7.79±3.61[a]	6.02±2.82[b]	4.18±2.15[b]	77.77±3.94[a]	90.84±8.12[b]	95.85±8.69[c]
Growing season SPEI≤-0.5	8.73±4.21[a]	6.09±2.74[b]	3.74±1.91[c]	80.55±4.96[a]	92.50±7.09[b]	98.36±9.02[c]
Non-growing season SPEI>-0.5	8.25±3.61[a]	6.30±2.70[b]	4.20±2.11[b]	78.13±4.34[a]	90.23±8.02[b]	96.30±9.18[c]
Non-growing season SPEI≤-0.5	7.95±4.25[a]	5.75±2.68[b]	3.83±2.05[b]	79.39±4.63[a]	92.77±7.36[b]	97.18±10.41[c]
VPD anomaly >0	9.02±3.43[a]	6.69±2.53[b]	4.419±1.86[c]	79.18±4.65[a]	92.00±7.49[b]	98.79±9.58[c]
VPD anomaly≤0	7.46±3.97[a]	5.59±2.87[b]	3.75±2.19[b]	78.39±4.40[a]	90.98±8.07[b]	95.24±9.63[c]

Colors in the column head from dark to light indicated decreasing trend of values of corresponding vigor class

The growing season expanded through April to September, and the non-growing season was defined as the period from previous October to the end of March in current year.

VPD anomaly was calculated as deviation of individual annual VPD value to the mean of the study period.

Different lower-case letters indicate significantly different means among vigor classes.

Abbreviations of health status: N: normal stands (no dieback tree); DI: stands of Dieback I degree (20-60% dieback trees); DII: stands of Dieback II degree (>60% dieback trees)

799 Table 3 Relationship between tree growth and monthly climatic variables

Growth variable	Vigor class	Climatic predictor	Previous year Jul.	Aug.	Sep.	Oct.	Nov.	Dec.	Current year Jan.	Feb.	Mar.	Apr.	May	Jun.	Jul.	Aug.	Sep.	Spectrum scale of Pearson coefficients
BAI	N	VPD																
		T																
		P																
	DI	VPD																
		T																
		P																
	DII	VPD																
		T																
		P																

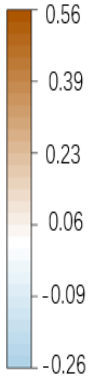

800 Pearson coefficients were reproduced to corresponding colors for the sake of clarity. Significant

801 correlation was highlighted with black frames.

802 Abbreviations of health status: N: normal stands (no dieback tree); DI: stands of Dieback I degree

803 (20-60% dieback trees); DII: stands of Dieback II degree (>60% dieback trees)

804

805

806

807 Table 4 Coefficients of predictors from the stepwise regression analysis summary over the

808 relationship between BAI and climatic variables (precipitation, *VPD*, c_a and T_c) in all vigor classes.

Dependent measure and factors entered		Ante-1997			Post-1997		
		N	DI	DII	N	DI	DII
Model included C_a	Constant	-124.758	-97.922	-69.33	57.467	55.156	54.395
	VPD	-0.367					
	c_a	0.374	0.295	0.21	-0.121	-0.124	-0.131
	Total R^2	0.974	0.97	0.864	0.628	0.726	0.718
Model excluded C_a	Constant	-2.946	-2.401	-0.985	9.688	6.347	
	T_c	0.237	0.198	0.131			
	SPEI				-1.794	-1.389	
	Total R^2	0.308	0.31	0.248	0.429	0.282	

809 *p<0.05; **p<0.01

810 Abbreviations of health status: N: normal stands (no dieback tree); DI: stands of Dieback I degree

811 (10-40% dieback trees); DII: stands of Dieback II degree (>40% dieback trees). Tc: cumulative

812 annual temperature

813 Ante- and Post-2000 stand for the study period before and after the year 2000, respectively.

814 publicity

815